International Journal of Industrial Electronics, Control and Optimization © 2020 IECO
Vol. 3, No. 4, pp. 415-429, Sep (2020)

Application of Improved Salp Swarm Algorithm Based on MPPT for PV Systems under Partial Shading Conditions

Javad Farzaneh[1], Ali Karsaz[2,†]

[1] Department of Electrical and Computer Engineering Faculty, Semnan University, Semnan, Iran
[2,†] Department of Electrical and Electronic Engineering, Khorasan Institute of Higher Education. Mashhad, Iran

ABSTRACT

Maximum Power Point Tracking (MPPT) is an important concept for both uniform solar irradiance and Partial Shading Conditions (PSCs). The paper presents an Improved Salp Swarm Algorithm (ISSA) for MPPT under PSCs. The proposed method benefits a fast convergence speed in tracking the Maximum Power Point (MPP), in addition to overcoming the problems of conventional MPPT methods, such as failure to detect the Global MPP (GMPP) under PSCs, getting trapped in the local optima, and oscillations around the MPP. The proposed method is compared with original algorithms such as Perturbation and Observation (P&O) method (which is widely employed in MPPT applications), Differential Evolutionary (DE) algorithm, Particle Swarm Optimization (PSO), and Firefly Algorithm (FA). The obtained results show that the proposed method can detect and track the MPP in a very short time, and its accuracy outperforms the other methods in terms of detecting the GMPP. The proposed ISSA algorithm has a higher speed and the convergence rate than the other traditional algorithms.

Article Info

Keywords:
Improved Salp swarm algorithm, Photovoltaic systems, Maximum power point tracking, Partial shading condition.

Article History:
Received 2019-08-16
Accepted 2020-06-30

I. INTRODUCTION

On account of restrictions on fuel resources, increased fossil fuel price, effects of fossil fuel sources on the environment and increased energy consumption, employing Renewable Energy Sources (RESs) has significantly increased during the last decades [1]. Among RESs, solar energy and Photovoltaic (PV) systems have greatly been utilized as they generate reliable electrical energy without producing emissions [2-3].

PV systems are considered as a reliable source of electrical energy generation thanks to the following reasons: they can be utilized widely all over the globe, they do not require fuel for energy generation, and their maintenance cost is very low [4]. Specific features, such as no depreciation and the minimum number of moving parts, have resulted in exclusive advantages for PV systems, including durability and increased lifelong up to roughly 20 years. Another advantage of PV systems is that they can be used in different capacities. Therefore, it is possible to supply the required energy of a residential home in small dimensions or even supply the needs of a town. Furthermore, the application of PV systems is economically feasible for supplying electrical energy in places where it is either impossible to transfer the electricity from the grid or when high amounts of time and cost should be invested. One major hurdle in employing PV systems is the high installation cost and low energy transformation efficiency, where the latter is somehow due to the nonlinear characteristics and

†Corresponding Author: karsaz@khorasan.ac.ir
† Department of Electrical and Electronic Engineering, Khorasan Institute of Higher Education. Mashhad, Iran

dependency of I-V and P-V characteristics on temperature and solar irradiance. Solar irradiance and temperature have direct bearings on the generated current and voltage of the PV system, respectively. Therefore, it is incumbent on us to employ MPPT technology in PV systems to extract the maximum power under different irradiance and temperature conditions [5]. Up to date, different methods have been introduced for MPPT under uniform insolation conditions, such as Perturbation and Observation (P&O) [6], Incremental Conductance (IC) [7], Fuzzy Logic-based methods [8], Artificial Neural Network (ANN) [9], Fractional Open-Circuit Voltage or Short-Circuit Current methods [10], and Hill Climbing (HC) [11]. The mentioned methods have great ability in MPPT applications under uniform insolation conditions. Among these methods, P&O and IC have the most extensive applications in comparison with the other mentioned methods [12]. In addition to temperature and irradiance, the other effective factor on the generated power of PV systems is the Partial Shading Condition (PSC). When PSC occurs due to the presence of clouds, shadings by trees, and or other objects in the neighborhood of the PV system, the output power of a PV system dramatically decreases. Normally, bypass diodes are used for reducing the PSC effect. If the bypass diodes are used in the case of PSC, the P-V characteristics curve of a PV system will have several peaks instead of one single peak. In this situation, conventional methods are unable to detect the GMPP and normally trap in the local optima [13].

Many different methods have already been introduced for MPPT under PSCs, all of which have their advantages and disadvantages. Among the available MPP tracking methods, optimization algorithm-based methods such as Firefly Algorithm (FA) [20], Particle Swarm Optimization (PSO) algorithm [14], Cuckoo Search (CS) algorithm [15], Ant Colony Optimization (ACO) algorithm [16], Grey Wolf Optimization (GWO) algorithm [17], Artificial Bee Colony (ABC) [18], Bat Algorithm (BA) [19], evolutionary algorithms [20], and Gravitational Search Algorithm (GSA) [21] are widely used. The reason behind this is that these types of techniques have many features, including the ability to detect the GMPP under any conditions, very small probability of trapping in the local optima, no oscillation around the MPP, and easy implementation in comparison to other methods.

Ref. [22] used the FA method for MPPT under PSCs, where a boost converter was utilized for connecting the load to the PV system. The method was compared with PSO and P&O methods, and it has been observed that the FA method has faster speed and higher accuracy in detecting the GMPP compared to the other two methods. A combined method was introduced in [16] for the MPPT application. In the first step, using an ACO algorithm, the proposed method reaches the neighborhood of the MPP and then tracks it by using the P&O method. GWO algorithm was employed in [23] for MPPT under PSCs. The author has compared the proposed method with P&O and other improved PSO methods and showed that the proposed method has a higher convergence speed without oscillations around the MPP. The average efficiency of the method is 99.85%. Fibonacci series was employed as a method of tracking the GMPP [24], where it was utilized as a mathematical basis for dividing the P-V curve. Since the method works based on a mathematical basis, it has very suitable accuracy, although its implementation cost is high. In [25], a method similar to the two-step search approach was used for MPPT under PSC. In this method, at first, the P-V curve is completely swept and the local optimum points are stored. Then, by perturbing the voltage and observing the power variations, the GMPP is tracked. The speed of this method is acceptable and has suitable tracking accuracy. An Adaptive Neuro-Fuzzy Inference System (ANFIS) was used for MPPT under uniform solar irradiance [26]. The suggested method has a very high convergence speed, and the accuracy of the MPPT depends on the learning quality of the ANFIS system such that if it is trained with enough data, it will have good accuracy. A new MPPT method based on the PSO algorithm was presented in [27], where extra coefficients are added to the PSO equations to reduce the computational effort of the algorithm. Nonetheless, it cannot be surely said whether the algorithm succeeds in continuously tracking the MPP. The reason is that when the particles are close to the MPP, the speed of the algorithm becomes significantly low or even is zero. One of the most common problems with the PSO algorithm is that when there is a small difference in the solar irradiances, the changes in the duty cycle should be small enough to be able to perform MPPT more accurately.

Ref. [28] makes use of the PSO algorithm for MPPT under PSC. In this paper, a boost converter is utilized for increasing the efficiency of the system for each solar panel, but this leads to the increased capital cost. Additionally, [29] used PSO for MPPT under PSCs. The author defined linear equations for parameters of the PSO algorithm to increase the speed and accuracy of the MPPT. The equations were tuned so that the system would have higher exploration and diversity at the beginning of running the algorithm, and the exploration value is decreased through running the algorithm so that the solutions converge. In [30], the ACO algorithm was used for MPPT. ACO is an inspiration by ant behaviors in the colony and the foraging path. The population size was assumed to be four. The proposed method was compared with PSO, P&O, and fractional open-circuit voltage methods. The simulation results were obtained for four different case studies of PSCs, highlighting the superiority of the ACO-based method over the other three methods. The authors in [31] combined the P&O algorithm with the genetic algorithm (GA) structure. This resulted in a reduction in the population size of the algorithm. Due to the reduction in the number of iterations (NOI), the

MPPT's speed increased significantly. In [32], a combined method was used for MPPT under PSCs. Noting that the P&O method is unable to detect the global optimum and the probability of trapping in the local optima is high, the author used it in conjunction with the PSO algorithm. In this method, at first, the P&O method starts the search process and once it reaches the local optimum point, the PSO method takes action. Since the P&O method is used in the first stage, it reduces the search space for the PSO method; thus, the system converges in a short time. A combination of PSO and P&O methods was employed in [33] for MPPT applications, where the P&O method is used under uniform solar irradiance and the PSO algorithm for tracking the MPP only at the beginning of PSCs. In ref. [34], by mixing the GWO and P&O methods, the author made an effort to extract the MPP under PSCs. Initially, the range of GMPP is determined by the GWO algorithm, and then the MPP is tracked using the P&O method. The speed of this approach is acceptable. In [35], the author has made some modifications in the FA method to reduce the convergence time while increasing the tracking speed of the MPPT. In this paper, using the average coordination of all fireflies as a representative point, the desired firefly moves only towards their average, instead of moving towards each of the brighter fireflies. In this method, by reducing the number of firefly movements, the tracking speed is increased. Nonetheless, the probability of not detecting the global optimum by the system is increased because the variety of fireflies' movements has dramatically reduced.

Li, Hong, et al. have proposed an overall distribution PSO and MPPT algorithm for a PV power system to track the GMPP under PSCs [36]. The main difference between our methodology and this new published paper is that in our algorithm the new proposed metaheuristic method SSA is used. The SSA is able to explore the most promising regions of the search space, move salps abruptly in the initial steps along with move gradually in the final steps of iterations compared to the standard and improved versions of the PSO methods. Moreover our proposed algorithm based on SSA method ensures and improves the average fitness of all salps, and enhance that best solution found so far over the course of optimization.

Recently, Yang, Bo, et al. proposed a new hybrid algorithm based on memetic algorithm and salp swarm optimization, named as MSSA [37]. The Memetic algorithm has developed into a broad class of algorithm and can properly hybrid a population based global search and heuristic local search. So the new ideal in this paper is to adopt the memetic computing framework to enhance the search ability of SSA, which mainly contains two operations, "local search in each chain" and "global coordination in virtual population". Therefore, this paper is also proposed a new method to improve the standard SSA as well as our methodology. In our proposed algorithm with a simple manner, contribution of previous position of salp to update new positions have increased. So our proposed algorithm is an alternative algorithm to Yang, Bo's idea in a simple manner.

The present work aims to use an improved salp swarm algorithm (ISSA) for the MPPT under PSCs in PV systems. The proposed method is compared with its counterparts, including the SSA method; the P&O method, which is a common method for MPPT; the DE method, which is one of the mostly-used evolutionary algorithms in engineering sciences and MPPT applications; and FA, and PSO methods, which work based on swarm intelligence and have suitable efficacy in tracking the MPP. It is worth mentioning that the optimization methods at the start of the algorithm are initialized randomly and the probability of trapping in the local optima is very high. Another challenge that should be investigated is the ability to detect the global optimum, which cannot be perceived or detected in only one or two times of executing of the simulation software. Thus, the suggested method is compared with DE, FA, PSO, and SSA methods by running the software for many times and the obtained results verify the superiority of the proposed method over its counterparts. The advantages of our proposed scheme make it different from some other works are:

1- The proposed ISSA benefits from many interesting features, making it a highly reliable method for accurate track of the MPP within a short time.

2- The ability to detect the global optimum, which cannot be perceived or detected in only one or two times of executing of the simulation software.

3- The proposed ISSA algorithm has a higher speed and converges very fast.

In the rest of the paper, the model of the solar cell, the effects of temperature and solar irradiance, as well as the effect of shading conditions on PV systems are given in Section II. In Section III, the objective function and the P&O method are described. SSA and ISSA methods are explained in Section IV, and their applications in MPPT are described. The simulation results are thoroughly presented in Section V and finally, conclusions are included in Section VI.

II. CHARACTERISTIC OF THE PV SYSTEM AND THE EFFECTS OF PSCS

A. *Modeling of the PV module*

A current source connected in shunt to a diode can be used to represent the equivalent circuit of an ideal PV cell. A resistor (R_p) is connected in parallel to the equivalent circuit to limit the leakage current flow. Similarly, a series resistor (R_s) is employed to measure the losses. There are two types of modeling for the PV cell: (i) single-diode model, and (ii) double-diode mode [38]. Between these two models, the later

is more accurate, but more parameters are required to accurately model the PV cell. As a result, a single-diode model is used in this paper for simplification. Fig. 1 illustrates the schematic of the single-diode model.

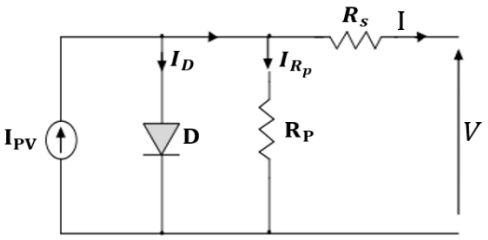

Fig. 1. Equivalent circuit of the single-diode model.

In general, equations of the output voltage and current of a solar cell are expressed as (1).

$$I = I_{PV} - I_O \left[exp\left(\frac{V+R_S I}{V_t a}\right) - 1\right] - \frac{V+R_S I}{R_P} \quad (1)$$

Where I_{PV} is the PV current and I_0 is the reverse saturation current. I_{PV} is defined based on the following equation:

$$I_{PV} = \left(I_{PV,n} - K_I \Delta T\right)\frac{G}{G_n} \quad (2)$$

The generated current due to solar irradiance at standard conditions (temperature of 25℃ and irradiance of 1000W/m^2) is $I_{PV,n.}$. In addition, ΔT is the temperature difference between the actual temperature (T) and the ambient standard temperature (T_n). K_I indicates the temperature coefficient of the short-circuit current. G is the irradiance and G_n denotes the irradiance at nominal conditions. Furthermore, for the inverse saturation current, we have:

$$I_o = \frac{I_{sc,n}+K_I \Delta T}{exp\left(\frac{V_{oc,n}+K_V \Delta T}{a V_t}\right)-1} \quad (3)$$

The short-circuit current and open-circuit voltage at nominal conditions are expressed by $I_{sc,n}$, $V_{oc,n}$,, and the voltage factor of the open-circuit is defined as K_V. The heating voltage of a panel with N_s number of solar cells connected in series is stated as (4).

$$V_t = \left(\frac{N_S K T}{q}\right) \quad (4)$$

q is the electron charge ($q = 1.6\, exp\,(-19)c$), k is the Boltzmann factor ($k = 1.3805 \exp(-23)\frac{j}{k}$), and T is cell's temperature in Kelvin.

B. *Effects of temperature and irradiance on the PV panel*

Characteristics of the assumed PV panel for this study at standard conditions (temperature = *25°C*, air mass = *1.5*, irradiance =1000 W/m^2) are given in Table.1. One of the effective factors of the produced power by PV systems is irradiance. By increasing solar irradiance, the produced power is proportionally increased, and vice versa. Fig. 2(a) depicts I-V and P-V curves of the PV panel under-study (MSX-60). As it is obvious from the figure, in the temperature of 25℃, when the irradiance is increased from 400 W/m^2 to 1000 W/m^2 with steps of 200, the generated current is increased and this entails the increase in the produced power. Besides, the temperature is also effective on the generated power by PV systems. By increasing temperature the output power is decreased, and vice versa. Fig. 2(b) illustrates that when the temperature is increased from 25℃ to 55℃ in the steps of 10℃, the open-circuit voltage is decreased, and as a result, the output power of the solar panel will decrease. Solar irradiance in graphs of Fig. 2(b) is assumed to be constant, equal to 1000 W/m^2.

Table. 1

Parameters of the MSX-60 PV module at STC

Maximum power (W), P_{MPP}	*60*
Nominal open-circuit voltage (V), V_{ocn}	*21.1*
Maximum power voltage (V), V_{MPP}	*17.1*
Nominal short-circuit current (A), I_{scn}	*3.8*
Maximum power current (A), I_{MPP}	*3.5*
Number of series cells, N_s	*36*

C. *Effects of PSCs on PV systems*

The produced power by a PV system depends on temperature and irradiance, and these two factors have direct impacts on the output power produced by the PV system. Another effective event on PV systems is PSCs. When a PV system is used in urban environments, PSC is not negligible. In most cases, the reason for the occurrence of PSC is the presence of trees, buildings, and other objects around PV systems. Hence, the impact of PSCs on the PV system should be investigated. When a part of a module or even the whole module of a PV system is under shading conditions, the output power reduces. In Fig. 3, the PV module has n cells. And a cell separated from the other cells is shown, which has current I and voltage V.

a)

b)

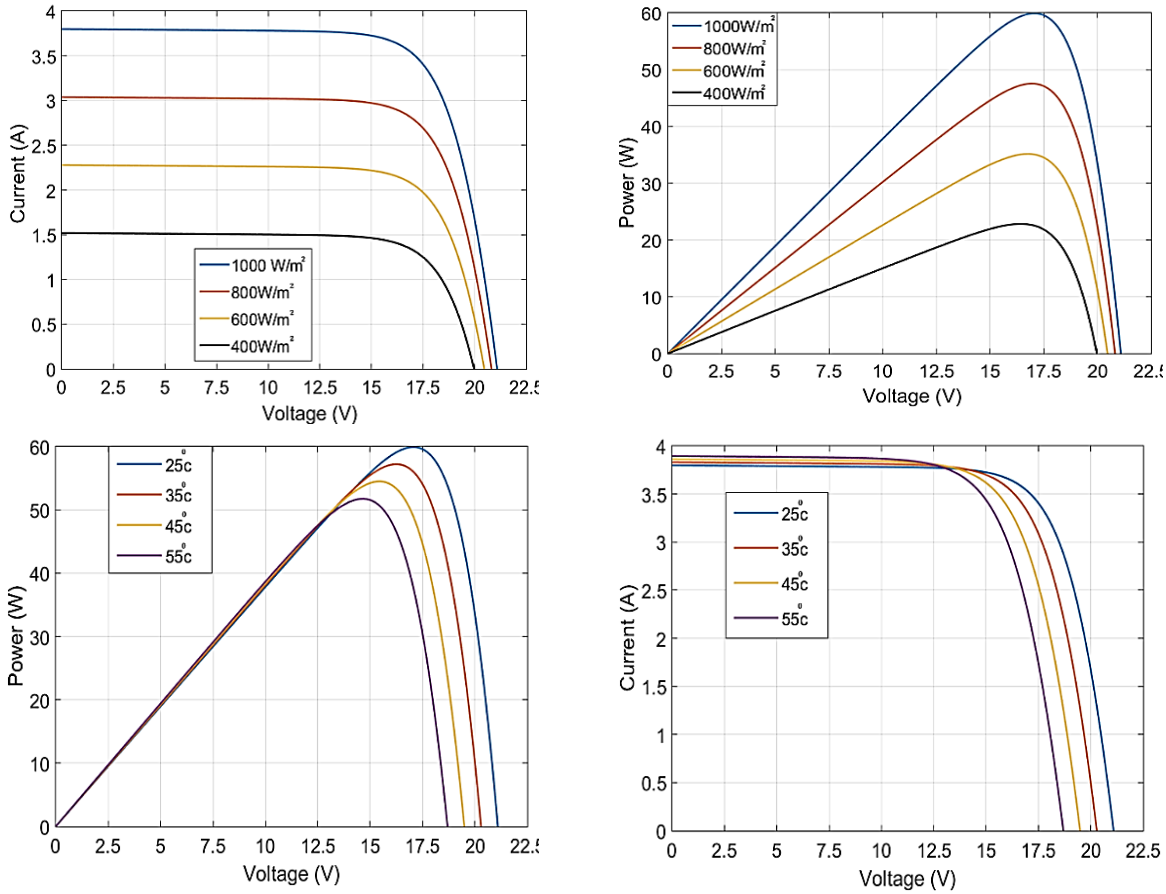

Fig. 2. The P-V and I-V curves under varying irradiation (b) The P-V and I-V curves under variable temperature

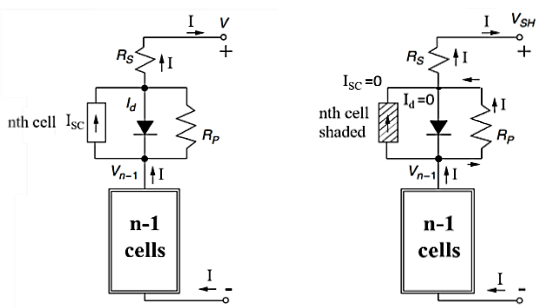

(a) (b)

Fig. 3. The PV module with n cells (a) all the cells are under solar irradiation, and (b) a cell under shading and n-1 cells under solar irradiation.

In Fig. 3 (a), all cells are under direct solar irradiation and are connected in series. Thus, the same current I is flowing through them. In Fig. 3(b), the upper cell is under shading condition and its produced current is zero. The remaining n – 1 cells are under solar irradiation. As a result, the whole current produced by n – 1 cells must flow through resistors R_p and R_s, and this reduces the output power. In the cases the PV modules are connected in series or shunt to increase the output power, bypass diodes are used to reduce the impact of PSCs. For instance, when PSC occurs and a module is under shading condition, diodes prevent the loss of power produced by other modules and impede the creation of a hotspot. Consequently, only the module under shading condition produces less power. P-V characteristics of PV systems differ in the presence and absence of the bypass diodes. Under shading conditions, different currents flow through the modules, therefore the P-V curve has several peaks. In Fig. 4, four PV panels are connected in series, wherein Fig. 4(a) the irradiance is the same for all panels and is equal to 1000 W/m^2. In Fig. 4(b), it is assumed that the PSC has occurred and irradiance is 1000 W/m^2, 850 W/m^2, 700 W/m^2, and 300 W/m^2, respectively. Fig. 5 depicts P-V and P-I curves in the presence of bypass diodes in the PV system of Fig. 4. As it is evident from Fig. 5, the uniform irradiance is equal to 1000 W/m^2, the produced power is 240 W. Moreover, when the PSC occurs, there are several peaks in the P-V curve and the produced power is decreased as well.

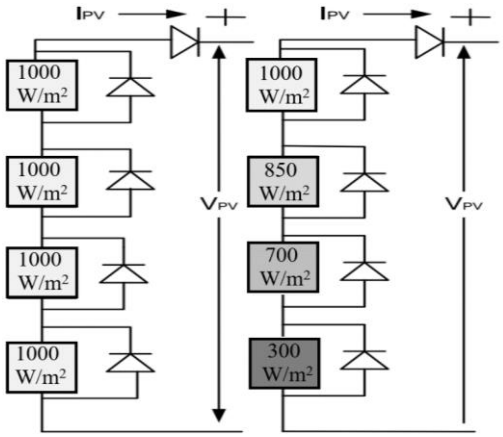

Fig. 4. A PV system with two different patterns.

(a)

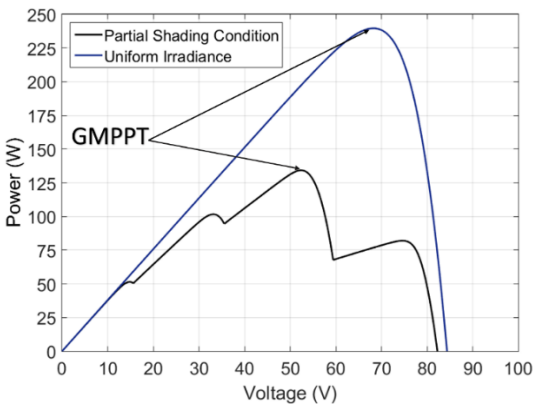

(b)

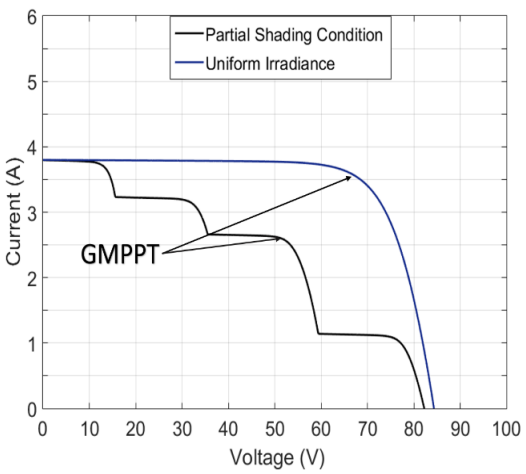

Fig. 5. The (a) P-V and (b) I-V curves of a PV system under uniform irradiance and PSCs.

III. OBJECTIVE FUNCTION AND P&O METHOD

The formulation of the MPPT as an optimization problem is as follows:

$$Maximize\ P_{pv}(d)$$
$$Subject\ to \begin{cases} d_{min} \le d \le d_{max} \\ V_{min} < V_{pv} < V_{max} \end{cases} \quad (5)$$

In Eq. (5), P_{PV} is the output power, d is the duty cycle of the DC-DC buck-boost converter, and d_{min} and d_{max} define the minimum and maximum duty cycles of the DC-DC converter. In this work, the latter two parameters are set *0.1* and *0.9*, respectively.

A. PERTURBATION AND OBSERVATION METHOD

The P&O method is a widely-used conventional method for MPPT under uniform irradiance as it has easy implementation and low cost compared with other MPPT methods [39]. In some papers, the P&O method is combined with other MPPT methods to increase the tracking speed [40]. The performance of the P&O method is such that, at first, a small controlled disturbance is established in the initial operating voltage of the PV system based on the tracking criteria. This is performed in such a manner that its value increases in case the produced power of the PV system is increased, i.e., the operating point moves toward the MPP. As a result, in the next disturbance, the operation voltage is established in the same direction exactly similar to the previous disturbance. This is continued until the MPP is reached. However, if the produced power by the PV system is reduced, it means that it has moved further away from the MPP. Therefore, the direction of the disturbance must be changed [41]. The efficacy of the P&O method is reduced by quick changes in environmental conditions and under PSCs because it is unable to track the GMPP under PSCs [42].

IV. SALP SWARM ALGORITHM

A. Inspiration and the proposed mathematical model

Salp swarm algorithm was introduced by Seyed Ali Mirjalli et al. in 2017 [42]. A swarm formed by a group of salps is known as a salp chain. The population of salps is divided into two groups to mathematically model salp chains: leader salp and follower salps. The leader salp is the one at the front end of the salp chain, and other salps are considered as followers. It is clear from the naming that the leader has the task of leading and guiding the followers. Like other population-based algorithms, an n-dimensional search space is assigned to define the positions of the salps, where n indicates the number of variables for a specific problem. A two-dimensional matrix, x, is used for storing the positions of the salps. Moreover, it is taken for granted that there is a food source, F, in the search space and the salp is trying to reach that. The following equation is used for updating the position of the leader salp:

$$x_j^1 = \begin{cases} F_j + c_1\left((ub_j - lb_j)c_2 + lb_j\right) & c_3 \ge 0 \\ F_j - c_1\left((ub_j - lb_j)c_2 + lb_j\right) & c_3 < 0 \end{cases} \quad (6)$$

It can be understood that the position of the leader is

updated only corresponding to F as the food source. In the above equation, x_j^1 is the position of the leader in the j^{th} dimension, F_j represents the food source in the j^{th} dimension, and ub_j and lb_j are the upper and lower boundaries of the j^{th} dimension. The most important parameter to be considered in the SSA is coefficient c_1 because this coefficient makes a random balance between exploration and exploitation. Furthermore, c_2 and c_3 are two random numbers generated uniformly in the interval [0, 1]. These two numbers determine the movement of the next position in the j^{th} dimension, either towards positive or negative infinity. Moreover, the size of the steps is defined by c_2 and c_3. The equation to update the position of the followers is:

$$x_j^i = \frac{1}{2}\left(x_j^i + x_j^{i-1}\right) \quad (7)$$

where $i \geq 2$ and x_j^i indicates the position of the i^{th} follower salp in the j^{th} dimension.

B. Improved SSA algorithm

In the SSA algorithm, the positions of the follower salps are updated based on (7). For the system to have a high convergence speed and converge within a shorter time, equation (7) is changed so that the previous positions of the follower salps have more contribution to updating new positions of the salps. This leads the salps to have smaller displacements with respect to their previous positions. According to (7) and assuming that x_j^i and $x_j^{i-1}$are positive values, (7) can be rewritten as:

$$x_j^i = \frac{1}{2}\left(x_j^i + x_j^{i-1}\right) = \frac{1}{2}\left((x_j^i + x_j^{i-1})^2\right)^{\frac{1}{2}} = \frac{1}{2}\left((x_j^i)^2 + (x_j^{i-1})^2 + 2x_j^i x_j^{i-1}\right)^{\frac{1}{2}} \quad (8)$$

In the above equation, for the contributions of previous positions of the salps have more effects on updating new positions, the value of $2(x_j^{i-1})^2$ is taken into account, not $2(x_j^i\, x_j^{i-1})$. As a result of this, the salps move less than their previous positions and finally, this increases the convergence speed. By simplifying (8), we have:

$$x_j^i = \frac{1}{2}\left((x_j^i)^2 + 3(x_j^{i-1})^2\right)^{\frac{1}{2}} \quad (9)$$

As it is clear from the above equation, contributions of previous positions of the salp to updating new positions have increased. Due to this, when the system will not experience large variations and have more inertia when reaches the optimal point, leading to increase convergence speed.

C. Application of the ISSA method to MPPT

In this section, the ISSA method is used for MPPT Fig. 6 shows the block diagram of the proposed system. The system under-study consists of four PV modules connected in series. Also, a buck-boost DC-DC converter is used as a link between the load and the PV system. In the following, the steps of the ISSA method for MPP tracking are illustrated in detail. Fig. 7 exhibits the flowchart of the proposed method.

Step 1: Adjusting the parameter c_1 of the ISSA and determining the population size, N. In this algorithm, the position of each salp is considered as the duty cycle of the buck-boost DC-DC converter. The power generated by the PV system is assumed as the fitness of each salp, which is corresponding to the position of each salp.

Step 2: Initialization of the salps. This step initializes the population of the salps in an acceptable solution space respect to the lower bound, d_{min}, and the upper bound, d_{max}. The position of a salp shows the duty cycle of the DC-DC converter. As was mentioned in the previous section, if the size of the population size large, the calculation time will increase; otherwise, the algorithm might be trapped in local optima. Therefore, the population size is assumed four, meaning that one salp for each panel.

Step 3: Fitness evaluation. In this step, the buck-boost converter operates sequentially corresponding to the position of each salp. For each duty cycle, the output power of the PV system is taken into account as the fitness of the corresponding salp. This step is repeated for positions of all of the salps available in the population.

Step 4: Updating salps' positions. The position of the leader salp is updated according to (6), and positions of the follower salps are updated based on (9).

Step 5: The termination criterion, similar to other optimization methods, is the number of iterations. Once it is reached, the algorithm stops, and the system operates based on the optimal duty cycle.

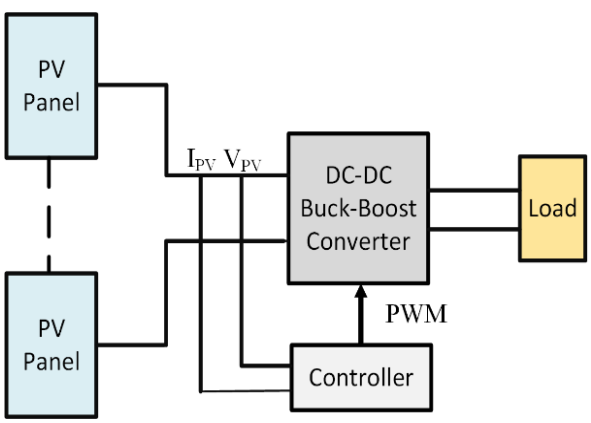

Fig. 6. Block diagram of the proposed system

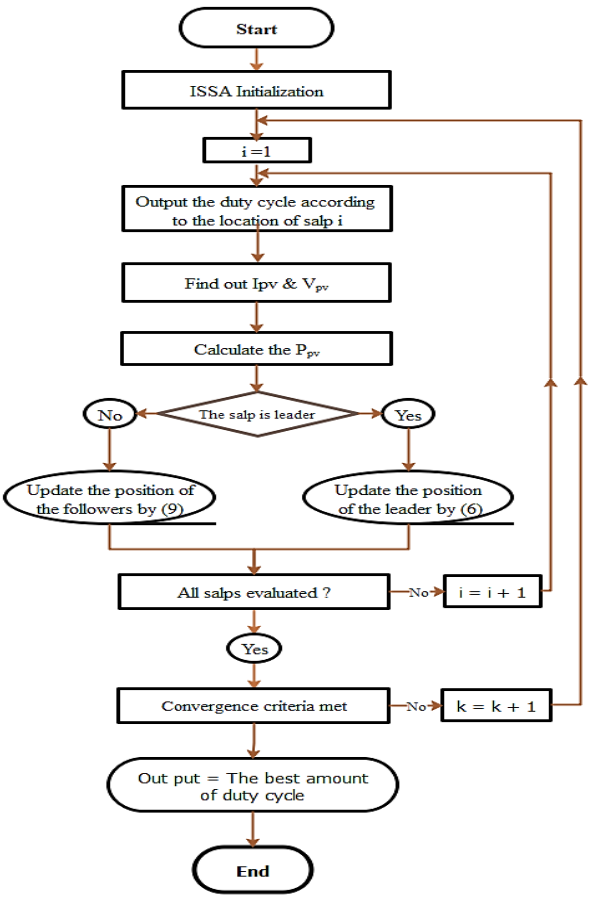

Fig. 7. Flowchart of the ISSA based MPPT

V. SIMULATION RESULTS

To analyze the global MPP tracking using the ISSA method, a thorough comparison is made between SSA; FA; and PSO methods; which work based on swarm intelligence; DE; and P&O methods, respectively. Extensive studies have been performed on MATLAB/Simulink software under different patterns of PSCs. The input inductance of the buck-boost DC-DC converter is 1 mH, the output capacitor is 220 µF, the input capacitor is 470 µF, and the switching frequency is 50 kHz. To ensure that the system will experience steady-state conditions before the start of the next particle to track the MPP, the sampling time interval is set 0.04 s. For the PSO method, C_1=1.2, C_2=1.6, and W=0.4 are taken into account, as in [28]. The number of iterations (NOI) is also set 10. The values of the FA parameter for (β_0, α, γ) are obtained by the trial and error method using simulations. Finally, the parameter values are given as β_0=2, α =0.6 and γ=1. Since each firefly moves towards the brighter ones, the NOI is set equal to 6 in the algorithm, yielding to shorter convergence time. Coefficients of the DE method are obtained by trial and error and using the FA parameters. To increase the convergence speed, parameter F is chosen randomly between 0.2 and 0.8, and CR=0.3. The NOI for this method is set 10. For the P&O method, T_a=0.005 (sampling interval), Δd=0.005 (magnitude of the disturbance on the duty cycle). For the SSA method, the constants of parameter c_1 are obtained by a trial and error method, and the new included coefficients are as follows:

$$c_1 = 3.2e^{-(\frac{3.5l}{L})^2} \quad (10)$$

Where l shows the present iteration and L represents the maximum NOI. For the ISSA method:

$$c_1 = 2.3e^{-(\frac{3.2l}{L})^2} \quad (11)$$

The values of NOIs in these two methods are set 10. The above-mentioned parameters are summarized in Table. 2.

Table. II
Parameters of the different methods used in this paper

PSO	C_1	1.2
	C_2	1.6
	W	0.4
	NOI	10
FA	β_0	2
	α	0.6
	γ	1
	NOI	6
DE	F_{Min}	0.2
	F_{Max}	0.8
	CR	0.3
	NOI	10
P&O	T_a	0.005
	Δd	0.005
SSA	c_1	$3.2e^{-(\frac{3.5l}{L})^2}$
	NOI	10
ISSA	c_1	$2.3e^{-(\frac{3.2l}{L})^2}$
	NOI	10

MPPT techniques have been used as controllers to supply the buck-boost converter with a desired duty cycle to study and compare dynamic responses of the PV system under PSCs. MPPT methods were investigated from the following perspectives: tracking time, convergence speed, oscillations around the MPP, and the efficiency of MPP tracking under PSCs. Two PSC patterns were utilized to evaluate the efficacy of the methods used in this paper in tracking the MPP. In the first PSC pattern, the irradiance on each module is 1000 W/m^2, 800 W/m^2, 600 W/m^2, and 400 W/m^2, respectively, and the temperature is set 25℃. P-I and P-V curves for the first PSC pattern and uniform irradiance (1000 W/m^2) are given in Fig. 8(a) and (b), respectively. In the first PSC pattern, there are four peaks, in which the GMPP is 116.468 W and is located on the P-I curve on the second peak. Details of the simulation results obtained for the PV system (power and duty cycle of the buck-boost converter) are provided in Fig. 9 for different MPPT techniques under the first PSC pattern.

a)

b)

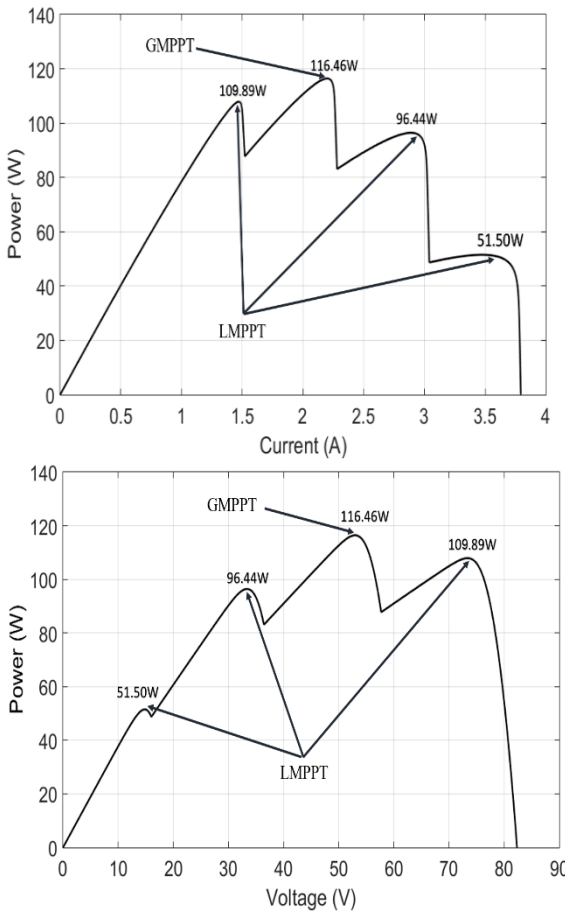

Fig. 8. (a) P−I curve (b) P−V curve under the first PSC

According to Fig. 9, the P&O method has reached a power of 108.5 W in less than 0.7 s. In terms of speed, the P&O method has acceptable speed but cannot detect the global MPP and is trapped in local optima. Further, power and duty cycle curves given in the corresponding curves of the P&O method are presented in smaller intervals to clearly show the changes in power and duty cycle. As is observed from the figure, duty cycle continuously changes in the P&O method and the output power has limited oscillation, which results in power loss. The FA method has succeeded to track the global MPP in less than 3 s and reach a power of 115.52 W. As is seen in the figure, the algorithm has tracked the global point in the last iterations and had changes when searching for the accurate point in the neighborhood of the optimal duty cycle. The algorithm continues its operation with the optimal duty cycle after the iterations are finished. Power and duty cycle curves in smaller intervals clearly show the convergence of the FA method. As is seen, the particles in the last iterations are seeking for the accurate MPP in the duty cycle range of 0.55. PSO, DE, and SSA methods track the GMPP within 1.76 s, 1.6 s, and 1.56 s, respectively. However, the ISSA method does it in a shorter time, within almost 1.2s. Compared to other methods, as is seen in Fig. 9, the ISSA method has successfully detected the GMPP in a very short time and extracted the maximum power. As the system tends to maintain its position in the proposed system, it converges with a high speed after detecting the considered point. Moreover, the suggested method benefits a significantly high accuracy. Simulation results are summarized in Table. 3. Also, to illustrate the impact of data uncertainties on the obtained solution, this table shows the results under 15 percent fluctuations in input data including temperature and irradiance for each panel.

Table. III
Performance comparison of P&O, PSO, and FA methods

Shading pattern	Technique	Power (W)	Tracking speed (s)	Power at the GMPP (W)	Voltage at the GMPP (V)	Current at the GMPP (A)	Tracking efficiency (%)
First case	P&O	108.5	0.76	116.46	53.95	2.16	92.44
	FA	115.52	2.92				99.01
	PSO	115.56	1.53				99.04
	DE	115.45	1.76				98.89
	SSA	115.58	1.35				99.12
	ISSA	115.59	1.22				99.13

P&O	a)	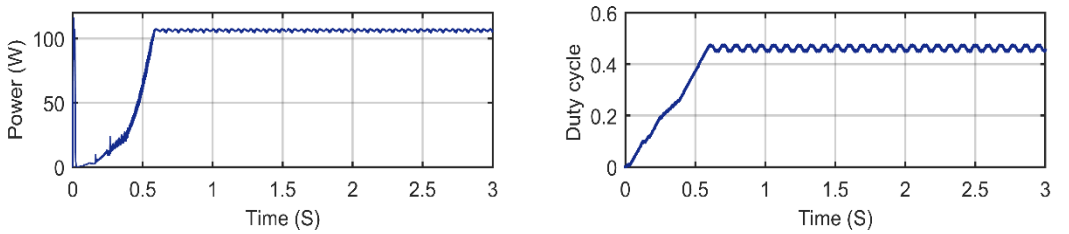
	b)	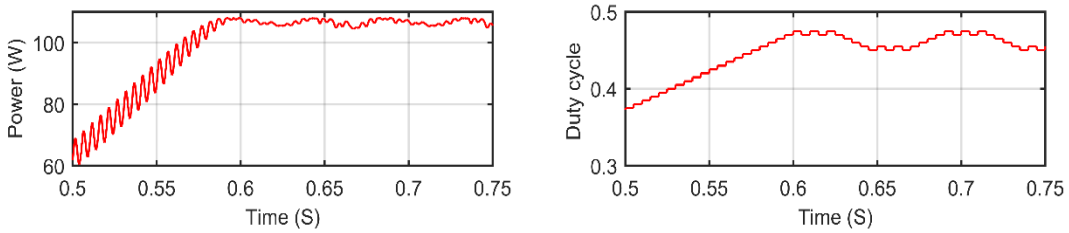
FA	a)	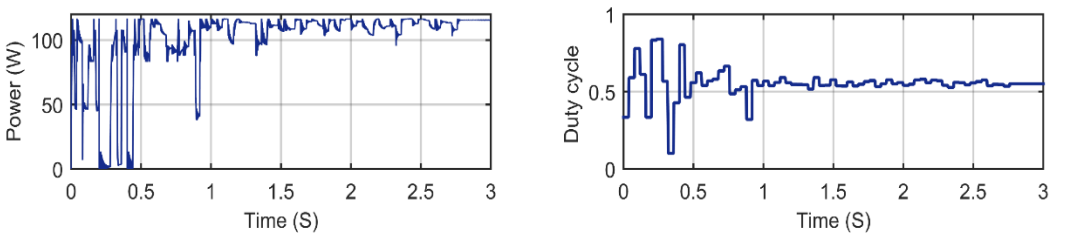
	b)	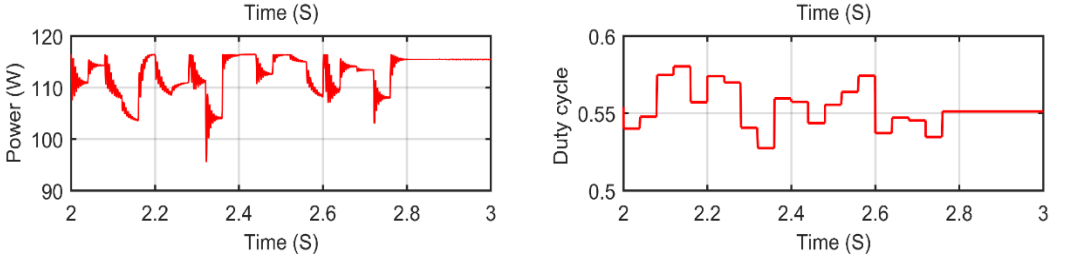
PSO	a)	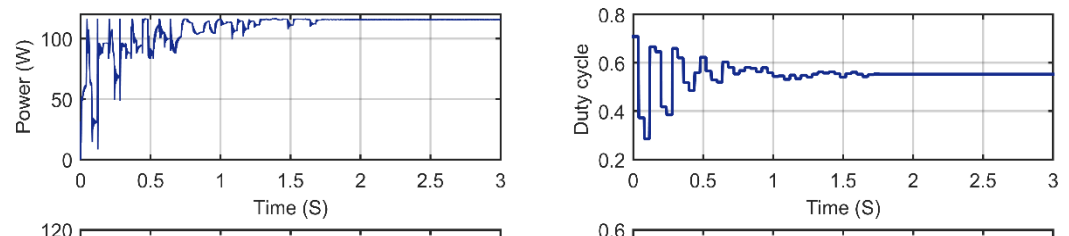
	b)	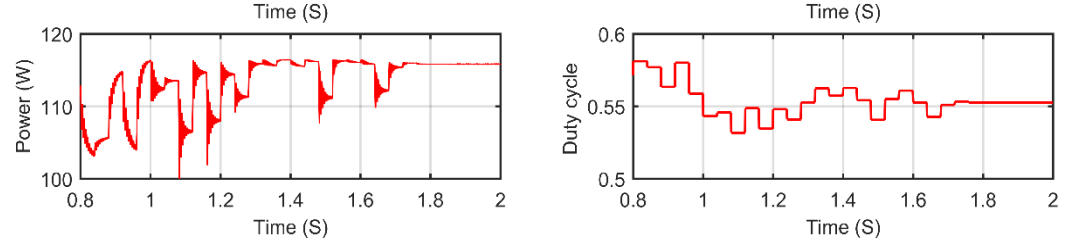

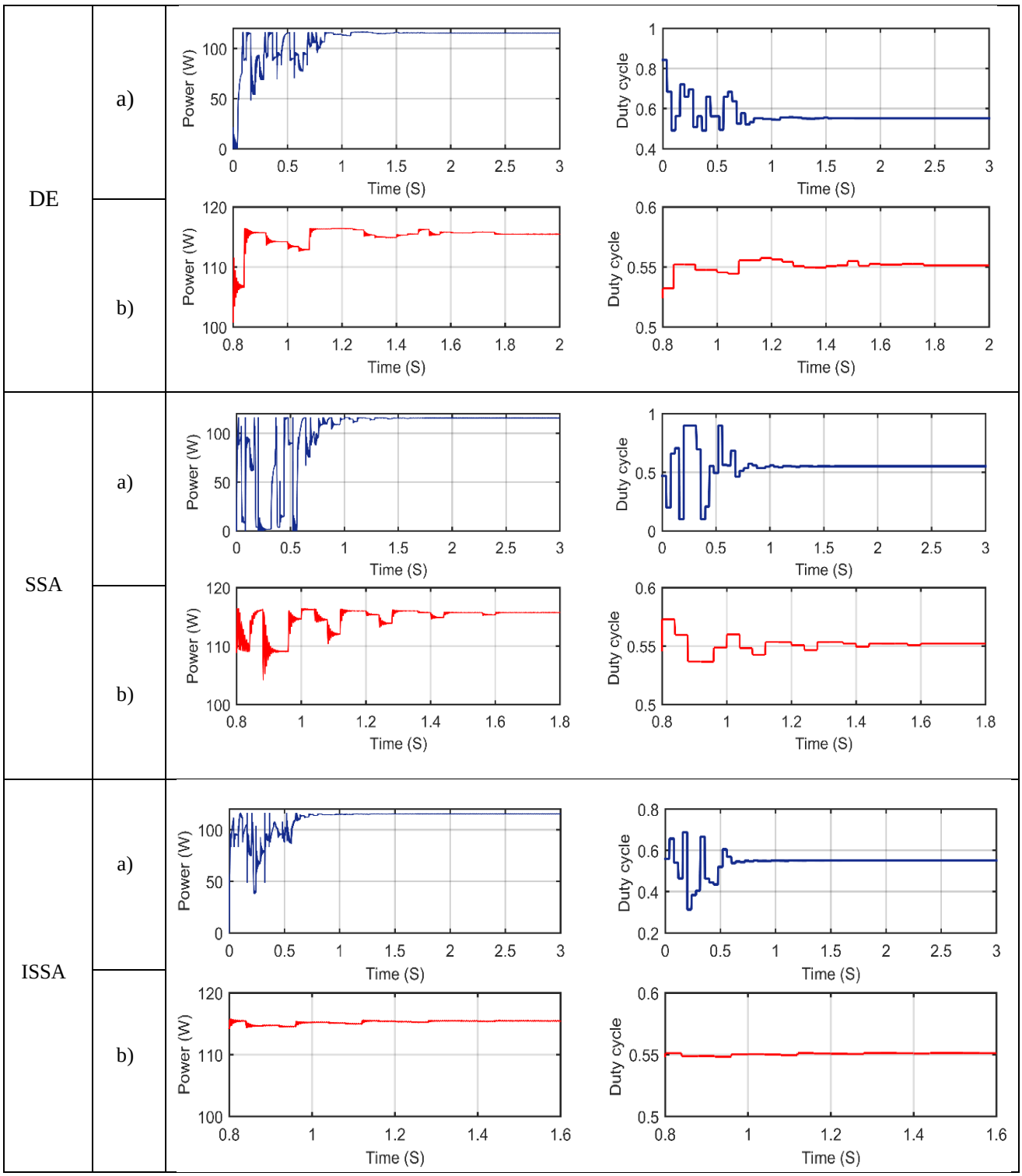

Fig. 9. Simulation results for the PV system under the first PSC, a) power and duty cycle curves, b) a with higher magnification

For further study, the second PSC pattern was also studied, in which the power difference between the global optimal point and one of the local optima is small to better show the efficiency of the algorithms. The irradiance for each panel is considered 1000 W/m^2, 800 W/m^2, 500 W/m^2, and 300 W/m^2, respectively, and the temperature is set 25℃. Another point that is worth noting here is that the efficacy of meta-heuristic algorithms cannot be proved only by one single run. Therefore, for the second PSC pattern, each algorithm was run 40 times to find the most efficient and superior MPP

tracking method under PSCs. P-I and P-V curves for the second PSC case are given in Figs. 10 (a) and (b), respectively. As observed in the P-V curve, the difference between the GMPP and one of the local optima is significantly small, making it difficult to detect the GMPP. The GMPP value is 98.21 W and the local optimal value with a small difference to the GMPP is 96.14W. It can be concluded from the obtained results of the first PSC case that the P&O method fails to detect the GMPP, and that is why it was not compared with other methods in the second PSC case. Details of simulation results obtained for the PV system from different MPPT methods under the second PSC case are shown in Fig. 11.

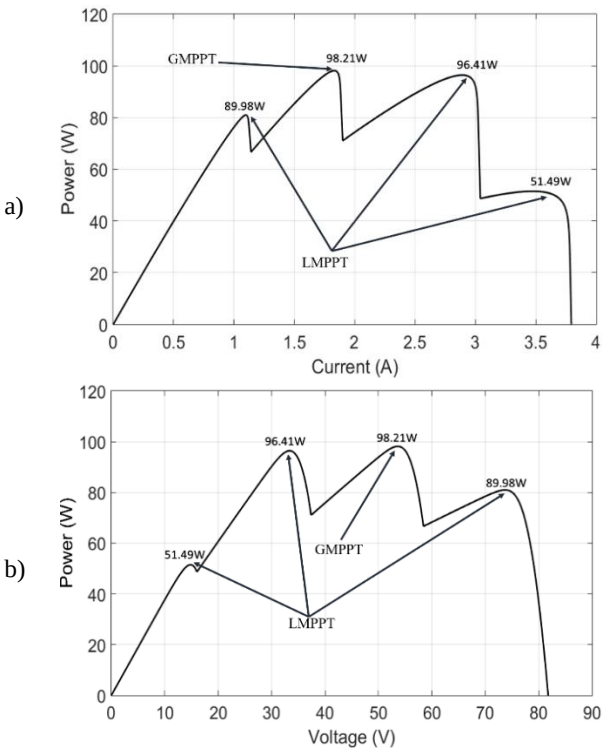

Fig. 10. (a) P−I curve (b) P−V curve under the second PSC

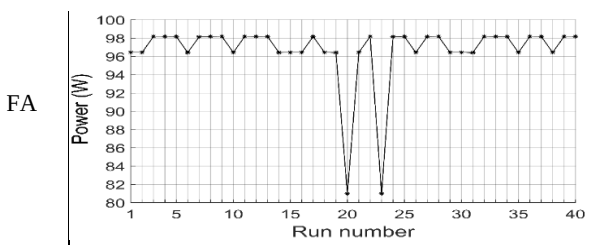

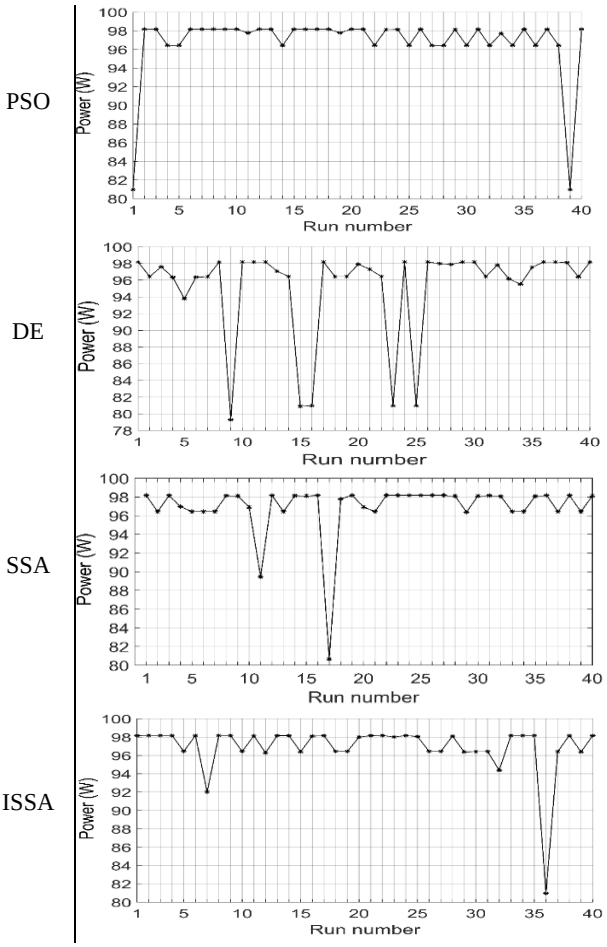

Fig. 11. Details of the PV system simulation results under the second PSC case.

In Fig. 11, meta-heuristic methods were compared from the MPPT ability point of view. As is evident in Fig. 11, the FA method was successful in tracking the GMPP for 22 out of 40 times, was trapped in a local optimum with a small difference to the GMPP for 16 times, and was trapped in other local optima for 2 times. These numbers for the PSO, DE, SSA, and ISSA methods were 23, 15, 2; 15, 20, 5; 24, 15, 1; and 24, 15, 1, respectively. Finally, from the first pattern of the PSC, it can be concluded that the ISSA method has a high convergence speed and is a suitable method for tracking the GMPP. According to the results obtained from the second PSC run for a high number of repetitions, notable conclusions can be drawn. The results of the second pattern show that the DE method is trapped in the local optima, so it cannot be considered as a reliable method. FA and PSO methods are more reliable than the DE method, and in most cases, they can detect the global optimum with satisfactory accuracy. Nevertheless, their convergence times are longer. Additionally, simulation results illustrate that SSA and ISSA methods have acceptable accuracy in detecting the GMPP. Table.4 describes a quality comparison between different

proposed methods.

Table. IV
Qualitative comparison of different methods

Criteria	ISSA	SSA	PSO	FA	DE	P&O
Periodic Tuning	Not Required	Not Required	Not Required	Not Required	Not Required	Not Required
Tracking Accuracy	Highly Accurate	Highly Accurate	Highly Accurate	Highly Accurate	Accurate	Low (may locate local peak)
Steady state oscillation	Zero	Zero	Zero	Zero	Zero	High
Tracking Speed (without PSC condition)	Fast	Medium	Medium	Medium	Medium	Very Fast
Ability to track under PSCs	High	High	High	High	Average	Poor
Algorithm complexity	Medium	Medium	Medium	Medium	Medium	Simple
Efficiency	High	High	High	High	Average	Poor in PSCs

VI. CONCLUSION

The original SSA algorithm is amongst the most recently introduced algorithms. In this paper, a new method based on the improved SSA is proposed for the MPPT under PSCs in PV systems. In this study, the method of updating the follower salps' positions is improved to increase the tracking speed of the MPP in the SSA algorithm. The ISSA method was compared with the original algorithm; the P&O method as a conventional method for MPPT; the DE method, which is included in evolutionary algorithms; and FA, and PSO methods as swarm intelligence algorithms, under PSCs. The simulation results obtained from MATLAB/Simulink software show that the proposed method, SSA, FA, PSO, and DE can track the GMPP under PSCs. In addition, ISSA and SSA methods have a noticeable capability in detecting the global MPP, even when the difference between the global optimum and the local optima is very small. Moreover, the speed of the ISSA method in tracking the GMPP under PSCs is higher than other methods. High efficiency and speed are the main advantages of the proposed method.

REFERENCES

[1] J. Zhao, X. Zhou, Z. Gao, Y. Ma, and Z. Qin, "A novel global maximum power point tracking strategy (GMPPT) based on optimal current control for photovoltaic systems adaptive to variable environmental and partial shading conditions," *Solar Energy*. Vol. 144 pp. 767–779, Mar. 2017.

[2] H. Rezk, M. Al-oran, M.R. Gomaa, M.A. Tolba, A. Fathy, M. Ali, A.G. Olabi, A.H.M. El-sayed, W. Addawaser, P. Sattam, B. Abdulaziz, and S. Arabia, *"A novel statistical performance evaluation of most modern optimization- based global MPPT techniques for partially shaded PV system,"* Renewable and Sustainable Energy Reviews, Vol. 115, Nov. 2019.

[3] J. Farzaneh, R. Keypour, and A. Karsaz, "A novel fast maximum power point tracking for a PV system using hybrid PSO-ANFIS algorithm under partial shading conditions," *International Journal of Industrial Electronics, Control and Optimization*, Vol. 2, No. 1, pp. 47-58, Nov. 2019.

[4] J. Farzaneh, R. Keypour, and M. Ahmadieh, *"A New Maximum Power Point Tracking Based on Modified Firefly Algorithm for PV System Under Partial Shading Conditions," Technology and Economics of Smart Grids and Sustainable Energy*, Vol. 3, No. 1, Jun. 2018.

[5] S. Titri, C. Larbes, K.Y. Toumi, and K. Benatchba, "A new MPPT controller based on the ant colony optimization algorithm for photovoltaic systems under partial shading conditions*," Applied Soft Computing*, Vol. 58, pp. 465–479. Sep. 2017.

[6] N. Femia, G. Petrone, G. Spagnuolo, and M. Vitelli, "Optimization of perturb and observe maximum power point tracking method, Power Electron*," IEEE transactions on power electronics*, Vol. 20, no. 4, pp. 963–973, Jul. 2005.

[7] Y. C. Kuo, T. J. Liang, and J. F. Chen, "Novel maximum-power-point-tracking controller for photovoltaic energy conversion system," *IEEE transactions on industrial electronics*. Vol. 48, no. 3, pp. 594–601, Jun. 2001.

[8] A. El Khateb, N.A. Rahim, and S. Member, "Fuzzy-logic-controller-based SEPIC converter for maximum power point tracking," *IEEE Transactions on Industry Applications*, Vol. 50, no. 4, pp. 2349–2358, Jan 2014.

[9] S. Saravanan, and N. R. Babu, *"RBFN based MPPT algorithm for PV system with high step up converter, Energy conversion and Management*," Vol. 122. pp. 239–251. Aug. 2016.

[10] M. a. S. Masoum, H. Dehbonei, and E.F. Fuchs, "Theoretical and experimental analyses of photovoltaic systems with voltage and current-based maximum power-point tracking," *IEEE Transactions on energy conversion*, Vol. 17, No. 4, Dec. 2002.

[11] E. Koutroulis, K. Kalaitzakis, and N.C. Voulgaris, "Development of a microcontroller-based, photovoltaic maximum power point tracking control system*," IEEE Transactions on power electronics*. Vol. 16, No. 1, PP. 46–54, Jan. 2001.

[12] A. Belkaid, I. Colak, and O. Isik, "Photovoltaic maximum power point tracking under fast varying of solar radiation," *Applied energy*. Vol.179, PP. 523–530, Oct. 2016.

[13] M. Farhat, O. Barambones, and L. Sbita, "A new maximum power point method based on a sliding mode approach for solar energy harvesting," *Applied energy*, Vol. 185, pp. 1185–1198, Jan. 2017.

[14] R. Aboelsaud, and S. Obukhov, "Improved particle swarm optimization for global maximum power point tracking of partially shaded PV array*," Electrical Engineering*, Vol. 101 NO. 2, pp. 443–455, Jun. 2019.

[15] J. Ahmed, and Z. Salam, "A maximum power point tracking (MPPT) for PV system using cuckoo search with partial shading capability*," Applied Energy*, Vol. 119, pp. 118–130, Apr. 2014.

[16] K. Sundareswaran, V. Vigneshkumar, P. Sankar, S.P. Simon, P. Srinivasa Rao Nayak, and S. Palani, *"Development of an improved P&O algorithm assisted* through a colony of foraging ants for MPPT in PV system," *IEEE Transactions on Industrial Informatics*, Vol. 12, No. 1, pp. 187–200, Nov. 2015.

[17] S. Mohanty, B. Subudhi, S. Member, and P.K. Ray, "A new MPPT design using grey wolf optimization technique for photovoltaic system under partial shading conditions*," IEEE Transactions on Sustainable Energy*, Vol. 7, No. 1, pp. 181-188, Oct. 2015.

[18] K. Sundareswaran, P. Sankar, P.S.R. Nayak, S.P. Simon, and S. Palani, "Enhanced energy output From a PV system under partial shaded conditions through artificial bee colony*," IEEE transactions on sustainable energy*, Vol. 6, No. 1, pp. 198-209, Nov. 2014.

[19] Z. Wu, and D. Yu, "Application of improved bat algorithm for solar PV maximum power point tracking under partially shaded condition," Applied Soft Computing, Vol. 62, pp. 101–109, Jan. 2018.

[20] M. Faridun, N. Tajuddin, and S. Ayob, "Evolutionary based maximum power point tracking technique using differential evolution algorithm," Energy and Buildings, Vol. 67, pp. 245–252, Dec. 2013.

[21] L. L. Li, G. Q. Lin, M. L. Tseng, K. Tan, and M. K. Lim, "A maximum power point tracking method for PV system with improved gravitational search algorithm," *Applied Soft Computing*, Vol. 65, pp. 333–348, Apr. 2018.

[22] K. Sundareswaran, S. Peddapati, and S. Palani, "MPPT of PV systems under partial shaded conditions through a colony of flashing fireflies," *IEEE transactions on energy conversion*, Vol. 29, pp. 463–472, Jan. 2014.

[23] S. Mohanty, B. Subudhi, and P.K. Ray, "A new MPPT design using grey wolf optimization technique for photovoltaic system under partial shading conditions," *IEEE Transactions on Sustainable Energy*, Vol. 7 No. 1, pp. 181–188. Oct. 2015.

[24] N.A. Ahmed, and M. Miyatake, "A novel maximum power point tracking for photovoltaic applications under partially shaded insolation conditions," *Electric Power Systems Research*, Vol. 78, No.5, pp. 777–784, May. 2008.

[25] B.N. Alajmi, K.H. Ahmed, S.J. Finney, B.W. Williams, and B. Wayne Williams, "A maximum power point tracking technique for partially shaded photovoltaic systems in microgrids," *IEEE Transactions on Industrial Electronics*, Vol. 60, No. 4, pp. 1596–1606, Sep. 2011.

[26] R.K. Kharb, S.L. Shimi, S. Chatterji, and M.F. Ansari, "Modeling of solar PV module and maximum power point tracking using ANFIS," *Renewable and Sustainable Energy Reviews*, Vol. 33, pp. 602–612, May. 2014,

[27] V. Phimmasone, T. Endo, Y. Kondo, and M. Miyatake, "Improvement of the maximum power point tracker for photovoltaic generators with particle swarm optimization technique by adding repulsive force among agents," *International conference on electrical machines and systems*, pp. 1-6, Nov. 2009.

[28] M. Miyatake, M. Veerachary, F. Toriumi, N. Fujii, and H. Ko, "Maximum power point tracking of multiple photovoltaic arrays: A PSO approach," *IEEE*

Transactions on Aerospace and Electronic Systems, Vol. 47, No. 1, pp. 367–380, Jan. 2011.

[29] Y. Liu, S. Huang, J. Huang, and W. Liang, "A particle swarm optimization-based maximum power point tracking algorithm for PV systems operating under partially shaded conditions," *IEEE Transactions on Energy Conversion*, Vol. 27, No. 4, pp. 1027-1035. Oct. 2012.

[30] L.L. Jiang, D.L. Maskell, and J.C. Patra, "A novel ant colony optimization-based maximum power point tracking for photovoltaic systems under partially shaded conditions," *Energy and Buildings*, Vol. 58, pp. 227–236, Mar. 2013.

[31] S. Daraban, D. Petreus, and C. Morel, "A novel MPPT (maximum power point tracking) algorithm based on a modified genetic algorithm specialized on tracking the global maximum power point in photovoltaic systems affected by partial shading," *Energy*. Vol.74, pp. 374–388, Sep. 2014.

[32] K.L. Lian, J.H. Jhang, and I.S. Tian, "A maximum power point tracking method based on perturb-and-observe combined with particle swarm optimization," *IEEE journal of photovoltaics*, Vol.4, No. 2, pp. 626–633, Jan. 2014.

[33] C. Manickam, G.R. Raman, G.P. Raman, S.I. Ganesan, C. Nagamani, A hybrid algorithm for tracking of GMPP based on P&O and PSO with reduced power oscillation in string inverters, *IEEE Transactions on Industrial Electronics*, Vol. 63, No. 10, pp. 6097–6106. Jul. 2016

[34] S. Mohanty, B. Subudhi, and P.K. Ray, "A grey wolf assisted perturb & observe MPPT algorithm for a photovoltaic power system," *IEEE Transactions on Energy Conversion*, Vol. 32, No. 1, pp. 340–347, Dec. 2016.

[35] D.F. Teshome, C.H. Lee, Y.W. Lin, and K.L. Lian, "A modified firefly algorithm for photovoltaic maximum power point tracking control under partial shading," *IEEE Journal of Emerging and Selected Topics in Power Electronics*, Vol. 5, No. 2, pp. 661–671, Jun. 2016.

[36] H. Li, S. Member, D. Yang, and W. Su, "An Overall Distribution Particle Swarm Optimization MPPT Algorithm for Photovoltaic System under Partial Shading," *IEEE Transactions on Industrial Electronics*, Vol. 66, No.1, pp. 265-275, Apr. 2018.

[37] B. Yang, L. Zhong, X. Zhang, H. Shu, T. Yu, H. Li, L. Jiang, and L. Sun, "Novel bio-inspired memetic salp swarm algorithm and application to MPPT for *PV systems considering partial shading condition," Journal of cleaner production*, Vol. 215, pp. 1203–1222, Apr. 2019.

[38] J.P. Ram, T.S. Babu, T. Dragicevic, and N. Rajasekar, "A new hybrid bee pollinator flower pollination algorithm for solar PV parameter estimation," *Energy conversion and management*, Vol. 135, pp. 463–476, Mar. 2017.

[39] V.R. Kota, and M.N. Bhukya, A novel linear tangents based P & O scheme for MPPT of a PV system, *Renewable and Sustainable Energy Reviews*. Vol. 71, pp. 257–267, May. 2017.

[40] K. Sundareswaran, V. Vignesh kumar, and S. Palani, "Application of a combined particle swarm optimization and perturb and observe method for MPPT in PV systems under partial shading conditions," *Renewable Energy*, Vol. 75, pp. 308–317, Mar. 2015.

[41] S. Lyden, and M.E. Haque, "A simulated annealing global maximum power point tracking approach for PV Modules under Partial Shading Conditions," *IEEE Transactions on Power Electronics*, Vol. 31, pp. 4171-4181, Aug. 2015.

[42] S. Mirjalili, A.H. Gandomi, S.Z. Mirjalili, S. Saremi, H. Faris, and S.M. Mirjalili, "Salp swarm algorithm: a bio-inspired optimizer for engineering design problems," *Advances in Engineering Software*, Vol. 114, pp. 163-191, Dec. 2017.

Javad Farzaneh was born in Mashhad, Iran, in 1991. He received the B.Sc. degree from the Bahar Institute of Higher Education, Mashhad, Iran, in 2014, the M.Sc. degree in electrical engineering from the Semnan University, Semnan, Iran, in 2017. His research interests are Artificial Neural Networks, Adaptive Neuro-Fuzzy Inference Systems (ANFIS), Stochastic Modeling and Estimation, System Identification, Soft Computing, Metaheuristic Optimization, Renewable Energy, Power Electronics.

Ali Karsaz received his B.S. degree in Electrical Engineering from the Amirkabir University of Technology (*Tehran Polytechnic*), Tehran, Iran, in 1999. He received his M.Sc. and Ph.D. degrees in Control Engineering both form Ferdowsi University of Mashhad, Iran, in 2004 and 2008, respectively. Since 2008, he has been Assistant Professor of control and biomedical engineering at Khorasan Institute of Higher Education and he was Chair of the Division of Control Department from 2012 until now. His current research interests include the development of mathematical models for analysis and control of Biological Systems, Pharmacodynamics, System Biology Mathematical Modeling, Artificial Neural Networks, Stochastic Modeling and Estimation, System Identification, Time Series Analysis and Prediction, Renewable Energy, Power Electronics, Inertial Navigation Systems, Multi-sensory Multi-target Tracking. He has published over 130 peer-reviewed articles in these and related research fields

IECO

This page intentionally left blank